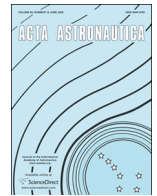




ELSEVIER

Contents lists available at ScienceDirect

Acta Astronautica

journal homepage: [www.elsevier.com/locate/actaastro](http://www.elsevier.com/locate/actaastro)

# Optimization of geosynchronous satellite constellation for independent regional navigation and positioning in Middle East region



Milad Asgarimehr\*, Masoud Mashhadi Hossainali

Department of Geodesy and Geomatics, K.N. Toosi University of Technology, Tehran, Iran

## ARTICLE INFO

### Article history:

Received 8 February 2014

Received in revised form

17 July 2014

Accepted 18 July 2014

Available online 1 August 2014

### Keywords:

Constellation design

Regional navigation satellite systems

Geosynchronous satellites

Genetic algorithm

Positioning satellite systems

## ABSTRACT

Regional Navigation and positioning systems using geosynchronous satellites are emerging for different parts of the world. Optimal constellation geometry achievement for a set of geosynchronous satellites is a key sector in designing of such systems. Genetic algorithm is applied for optimization of constellations with 6 and 7 satellites which is to be used in Middle East region where these systems have been deprived of. Based on the fact that the coverage criterion is not sufficient enough to guarantee a good navigation service, positioning process by the satellite systems is discussed and the performance of the system on the basis of position dilution of precision is collected as the fitness criterion. Placing the satellites in groups to pass over the same ground track is applied as a constraint to the genetic algorithm. By simulation, performance of the best obtained results and GPS are compared in terms of position dilution of precision, visibility and the required epochs (time span) to resolve the ambiguities with a 99% success rate, in this region. Also, capability of the GA for such problems is demonstrated.

© 2014 IAA. Published by Elsevier Ltd. All rights reserved.

## 1. Introduction

Global navigation satellite systems such as Global Positioning system (GPS) and GLONASS have successfully provided significant services in recent decades. Increased expectations of the positioning accuracy and its quickness as well as ongoing changes in the users' environment (i.e. the creation of urban buildings occasioning navigation signal blocks and the emergence of new applications requiring more precise positioning) confine the availability and capability of the current GNSSs' services. For example, mountainous terrain and urban canyons in Japan do not allow a clear skyline to the horizon. The Quasi-Zenith Satellite System (QZSS) is a Japanese regional satellite navigation system (when fully deployed) consisting of several QZSS Geosynchronous satellites placed in highly

inclined elliptical orbits (HEO). QZSS was authorized in 2002 to increase the availability of GPS in Japan's numerous urban canyons, where only satellites at very high elevation can be seen. A secondary function of this system is performance enhancement, increasing the accuracy and reliability of GPS derived navigation solutions. The system is designed so that at least one satellite is constantly located at a high elevation angle, thus the term 'quasi-zenith'. This is to ensure that one of the satellites is always visible near zenith over Japan. The Japan Aerospace Exploration Agency (JAXA) successfully launched the first QZSS satellite, 'Michibiki' (or QZS-1), on 11 September 2010. JAXA declared QZS-1 user-ready in June 2011. Three more satellites are commissioned to be launched by the end of 2017, bringing the constellation to three HEO satellites and one satellite in a Geostationary Orbit (GEO) [1].

In a quest for independence, Indian Space Research Organization (ISRO) has exclusively planned a yet-to-be-operational Indian Regional Navigational Satellite System (IRNSS) of seven geosynchronous satellites. The constellation

\* Corresponding author. Tel.: +98 9126431272.

E-mail address: [miladasgarimehr@gmail.com](mailto:miladasgarimehr@gmail.com) (M. Asgarimehr).

consists of three GEO satellites located at 34-deg E, 83-deg E and 132-deg E longitude, and four Inclined Geosynchronous Orbit (IGSO) satellites placed in orbits inclined at an angle of 29-deg with longitude crossings at 55-deg E and 111-deg E. These constellations along with the ground support will be operational by 2014 [2].

Moreover, China has designed and launched BeiDou with similar intentions. The nominal constellation of BeiDou Navigation Satellite (regional) System is composed of fourteen satellites, including five GEO satellites and nine Non-Geostationary Earth Orbit (Non-GEO) satellites [3]. The Beidou constellation has been completed in October 2012. It symbolizes that the construction of the Chinese independent navigation satellite system has entered a new development phase [4].

How to design a satellite constellation is one of the key sectors in the aerospace field of research. As a complementary or an independent regional navigation system, optimal constellation geometry for a set of geosynchronous satellites must be achieved in the design process. Constellation design is a typical multiple peaks, multiple valleys and non-linear multi-objective optimization problem. The goal is to find a set of parameters in order to form a constellation which covers the desired area, not only to provide the optimal performance, but also to save the operational cost. The multi objective Genetic Algorithm (GA) has been introduced as a robust technique to solve many multivariable problems [5,6]. Optimum Satellite constellation has been resolved for various missions based on different criteria by GA [7–11].

Usually, the constellations are selected with the help of an optimization criterion based on the satellite visibility from the users. A good zonal or global coverage is needed for the constellation of a communication satellite system. But, even if it can provide good insights, the coverage criterion is not sufficient enough to guarantee a good navigation service. Obviously it can provide the 4-fold coverage we need (it is well known that a minimum of four visible satellites is needed to compute position, velocity and time information), but it provides no indications about the geometrical layout of the satellites, as an important contributor to the positioning precision. This work uses the GA in order to optimize constellation geometry along with positioning accuracy parameters based on criteria, for an independent regional navigation satellite system using geosynchronous satellites. This system is supposed to be utilized in the Middle East region with longitudes from 25-deg E to 75-deg E and latitudes from 10-deg N to 45-deg N

Section 2 discusses on the adopted design criteria in this research. The fitness function, constraints and optimization process are given next in section 3. Section 4 discusses on the obtained numerical results.

## 2. Positioning by satellite navigation systems

We propose a criterion based on the positioning accuracy to optimize the constellation directly. To introduce this criterion, introduction of the positioning process is inevitable.

In general, the measured ranges from a positioning satellite to a receiver, by pseudo-range and carrier phase, respectively, can be written as a function of unknown parameters by use of the following generic measurement equations [12]:

$$P_{r,i}^s = \rho_r^s + d_{r,i} - d^{s,i} + \frac{f_1^2}{f_i^2} I_r^s + T_r^s + \epsilon_{r,i}^s \quad (1)$$

$$\Phi_{r,i}^s = \rho_r^s + \delta_{r,i} - \delta^{s,i} - \frac{f_1^2}{f_i^2} I_r^s + T_r^s + \lambda_i N_{r,i}^s + \epsilon_{r,i}^s \quad (2)$$

where  $P$  and  $\Phi$  are the code and carrier phase observations, respectively.  $\rho$  is the geometric range from satellite  $s$  to receiver  $r$ .  $i$  is the frequency signals of the positioning satellite;  $i = 1, \dots, NOS$ , where  $NOS$  is the number of frequencies utilized in the system.  $f$  is the frequency of the signals.  $I$  represents the ionospheric delay on  $i = 1$  frequency and  $T$  is the tropospheric delay,  $d$  and  $\delta$  are the clock error for code and carrier phase measurements, respectively.  $\lambda$  and  $N$  are the wavelength and the ambiguity parameter in cycles, respectively.  $\epsilon$  and  $\epsilon$  are the accumulated effect of receiver noises on the carrier phase and the pseudo-range, respectively.

### 2.1. Dilution of precision

Using only code observations, the measurements are linearized as [12]:

$$\delta P = G \begin{bmatrix} \delta x \\ \delta b \end{bmatrix} + \tilde{\epsilon}_p \quad (3)$$

where  $\delta P$  is a vector containing predicted minus actual code measurement as its components. Components of the vector  $\delta x$  are the position offsets of the user from the linearization point and  $\delta b$  is the offset of the user time bias.  $G$  is a  $(m \times 4)$  matrix characterizing the satellite-receiver geometry. The geometry matrix  $G$  only depends upon the relative position of satellites and the receiver.  $m$  is the number of measurements (depending on visible satellites and the number of adopted frequencies), and  $\tilde{\epsilon}_p$  is the vector of residual errors.

The Dilution of Precision (DOP) is a measure for the geometrical strength of the observation model. DOP can be expressed as a number of separate measurements. Geometric DOP (GDOP), Position DOP (PDOP), Horizontal DOP (HDOP), Vertical DOP (VDOP), and Time DOP (TDOP). The DOP factors are functions of the diagonal elements of the covariance matrix,  $Q = (G^T G)^{-1}$ . DOPs are defined as [12]:

$$GDOP = \sqrt{Q_{11} + Q_{22} + Q_{33} + Q_{44}} \quad (4)$$

$$PDOP = \sqrt{Q_{11} + Q_{22} + Q_{33}} \quad (5)$$

$$HDOP = \sqrt{Q_{11} + Q_{22}} \quad (6)$$

$$VDOP = \sqrt{Q_{33}} \quad (7)$$

$$TDOP = \sqrt{Q_{44}} \quad (8)$$

The Root Mean Square (RMS) of the three position errors,  $rms(x)$ , may thus be given as [12]:

$$rms(x) = \sigma_{URE} PDOP \quad (9)$$

Where  $\sigma_{\text{URE}}$  is the accuracy of the range measurements. Eq. (9) indicates that the achievable position accuracy depends on both the accuracy of the pseudo-ranges and the satellite-receiver geometry. The more favorable the geometry, the lower the DOP will be. The lower the DOP is, the higher the accuracy of the position estimate, in general. To evaluate the DOPs we need at least four visible satellites. But of course, if more satellites are available all the pseudo-range measurements will be used to compute the user location. However, it should be pointed out that the DOPs do not fit exactly with the real errors in the estimated user position for example, from one satellite to another the error budget often varies as a function of the atmospheric perturbations. But they still provide a useful measure of performance that takes into account the geometry of the satellites relative to the users. Therefore, it can be a useful criterion to optimize a satellite constellation for positioning purposes.

### 2.2. Carrier-phase-based positioning

The linearized double difference observations are collected in the following linear system of equations [12–15]:

$$\mathbf{y} = \mathbf{A}\mathbf{a} + \mathbf{B}\mathbf{b} + \mathbf{e} \quad (10)$$

where  $\mathbf{y}$  is the given data vector,  $\mathbf{y} \in R^m$ ;  $\mathbf{a}$  and  $\mathbf{b}$  are the unknown parameter vectors of order  $n$  and  $p$  respectively.  $\mathbf{A}$  and  $\mathbf{B}$  are respectively the corresponding design matrices of order  $m \times n$  and  $m \times p$ .  $\mathbf{e}$  is the noise and un-modeled effects vector of order  $m$ .

The data vector  $\mathbf{y}$  will usually consist of “observed minus compute” single-, dual-, or triple-frequency double difference carrier phase and/or code observations, accumulated over all observation epochs.  $\mathbf{a}$  denotes the vector of double difference ambiguities, expressed in unit of cycles rather than the range. They are known to be integers,  $\mathbf{a} \in Z^n$ .  $\mathbf{b}$  represents the vector that contains the increments of the  $p$  baseline components, double difference ranges in the case of the geometry-free model or baseline components in the case of the stationary receiver geometry-based model and the roving receiver geometry-based model. The entries of  $\mathbf{b}$  are known to be real values,  $\mathbf{b} \in R^p$ . It should be noted that other unknowns such as atmospheric delay parameters (troposphere, ionosphere) and/or other parameters of interest can be added to the system of equations as components of  $\mathbf{b}$ . Read more about the geometry-free model, stationary receiver geometry-based model and roving receiver geometry-based model in Refs. [16,17].

The procedure which is usually followed for solving the carrier phase based positioning model can be divided into three steps: the float solution, the integer ambiguity estimation and the fixed solution [18].

In the first step, the float solution, the integer constraints  $\mathbf{a} \in Z^n$  on the ambiguities is simply disregarded. In this step a standard least-squares adjustment is performed:

$$\min_{\mathbf{a}, \mathbf{b}} \|\mathbf{y} - \mathbf{A}\mathbf{a} - \mathbf{B}\mathbf{b}\|_{\mathbf{Q}_y}^2 \quad \text{with } \mathbf{a} \in R^n, \mathbf{b} \in R^p \quad (11)$$

where  $\mathbf{Q}_y$  is the variance-covariance matrix of the double difference observations  $\mathbf{y}$ . The real valued estimates and variance-covariance matrix will be obtained [14]:

$$\begin{bmatrix} \hat{\mathbf{a}} \\ \hat{\mathbf{b}} \end{bmatrix}, \begin{bmatrix} \mathbf{Q}_{\hat{\mathbf{a}}} & \mathbf{Q}_{\hat{\mathbf{a}}\hat{\mathbf{b}}} \\ \mathbf{Q}_{\hat{\mathbf{b}}\hat{\mathbf{a}}} & \mathbf{Q}_{\hat{\mathbf{b}}} \end{bmatrix} \quad (12)$$

In the second step, the integer ambiguity estimation, the float ambiguity estimate  $\hat{\mathbf{a}}$  is used to compute the corresponding integer ambiguity estimate  $\check{\mathbf{a}}$

$$\check{\mathbf{a}} = \mathbf{M}(\hat{\mathbf{a}}) \quad (13)$$

$\mathbf{M}$  is a mapping function from the  $n$ -dimensional space of real numbers to the  $n$ -dimensional space of integers, so  $\mathbf{M} : R^n \rightarrow Z^n$ . As this mapping and for computation of the integer estimate, LAMBDA method will be used. This method is discussed further.

In the third step, the fixed solution, the final solution will be obtained with the ambiguities fixed by (13):

$$\check{\mathbf{b}} = \hat{\mathbf{b}} - \mathbf{Q}_{\hat{\mathbf{b}}\hat{\mathbf{a}}} \mathbf{Q}_{\hat{\mathbf{a}}}^{-1} (\hat{\mathbf{a}} - \check{\mathbf{a}}) \quad (14)$$

As a result, the ambiguity resolved unknown parameters solution,  $\check{\mathbf{b}}$ , is obtained.

#### 2.2.1. Stochastic model

When the ionospheric parameters are considered as unknowns in the measurement equations, the variance-covariance matrix of the observations of one satellite is given as:

$$\mathbf{C}_{P\phi} = \begin{bmatrix} \mathbf{C}_P & \\ & \mathbf{C}_\phi \end{bmatrix} \quad (15)$$

where  $\mathbf{C}_P$  and  $\mathbf{C}_\phi$  are the variance-covariance matrices of the code and phase measurements, respectively. There may be correlations between the code and the phase observations on different frequencies. If the ionospheric parameters are eliminated from the measurement equations using pseudo-observables, the ionospheric delays will be treated as stochastic variables. The variance-covariance matrix of pseudo-observables can be written as:

$$\mathbf{C}_I = s^2 \begin{bmatrix} \boldsymbol{\mu} \\ -\boldsymbol{\mu} \end{bmatrix} \begin{bmatrix} \boldsymbol{\mu} \\ -\boldsymbol{\mu} \end{bmatrix}^T \quad (16)$$

where  $\boldsymbol{\mu} = (\mu_{i(1)}, \dots, \mu_{i(l)})$ ;  $l$  is the number of frequencies used for each solution and  $\mu_i = \lambda_i^2 / \lambda_1^2$ .  $s^2$  is the ionospheric weighting factor in units of square meters, which can vary between zero and infinity. When ionospheric delays are absent or assumed known,  $s^2 = 0$ , which may be the case when the baseline is sufficiently short. This is referred to as the ionosphere-fixed. For long baselines, when the ionospheric behavior is completely unknown, the ionosphere-float model should be used, which means that  $s^2 \rightarrow \infty$ . The value may vary between these two extreme values depending on baseline length, which is referred to ionosphere-weighted model. For more review see [18] and [19]. By introducing  $\mathbf{Q}$  as:

$$\mathbf{Q} = \mathbf{C}_{P\phi} + \mathbf{C}_I \quad (17)$$

The complete variance-covariance matrix of double difference observations is then given as [16]:

$$\mathbf{Q}_y = \mathbf{I}_k \otimes 2\mathbf{Q} \otimes \mathbf{E} \quad (18)$$

where  $\mathbf{E} = \mathbf{D}^T \mathbf{D}$ , and  $\mathbf{D}^T$  is the  $(m-1) \times m$  double differencing operator. The factor 2 stems from error propagation after taking the single difference. The notation  $\mathbf{I}_k$  denotes an identity matrix of order  $k$ ;  $k$  is the number of epochs used for each solution and  $\otimes$  denotes the Kronecker product.

### 2.2.2. Integer ambiguity estimation

Various methods (i.e., integer ambiguity estimators) for mapping  $\hat{\mathbf{a}}$  into  $\check{\mathbf{a}}$  have been proposed. An efficient method to resolve is the LAMBDA method [14,18]. This method consists of two steps. At first, the float ambiguities are decorrelated in order to eliminate the discontinuity in the spectrum of conditional variances. The discontinuity causes the search space to be elongated. Thereby, the adopted search algorithm for finding the correct integer ambiguities becomes inefficient in practice. So, the decorrelation makes the second step, the search for integers, much more efficient. Let the float solution be given as Eq. (12). The decorrelation matrix  $\mathbf{Z}^T$  transforms the ambiguities and their variance-covariance matrix into:

$$\check{\mathbf{z}} = \mathbf{Z}^T \hat{\mathbf{a}}, \quad \mathbf{Q}_{\check{\mathbf{z}}} = \mathbf{Z}^T \mathbf{Q}_{\hat{\mathbf{a}}} \mathbf{Z} \quad (19)$$

The elements of matrix  $\mathbf{Z}^T$  are all integers. This transformation preserves the volume of search space, i.e. its determinant must be  $\pm 1$ . The search step is then carried out to determine the integer values,  $\check{\mathbf{z}}$ , of the transformed ambiguities. The integer values of the ambiguities are obtained by the inverse transformation Eq. (19) as below:

$$\check{\mathbf{a}} = \mathbf{Z}^{-T} \check{\mathbf{z}} \quad (20)$$

Finally these ambiguities can be used to obtain the fixed solution of the baseline coordinates by Eq. (14). The precision of this baseline solution will be much better than the precision of the float solution. This can be seen by applying the propagation law of variances to Eq. (14) and assuming that the fixed ambiguities are non-stochastic parameters:

$$\mathbf{Q}_{\check{\mathbf{b}}} = \mathbf{Q}_{\hat{\mathbf{b}}} - \mathbf{Q}_{\hat{\mathbf{b}}\hat{\mathbf{a}}} \mathbf{Q}_{\hat{\mathbf{a}}}^{-1} \mathbf{Q}_{\hat{\mathbf{a}}\hat{\mathbf{b}}} \quad (21)$$

This shows that  $\mathbf{Q}_{\check{\mathbf{b}}} \ll \mathbf{Q}_{\hat{\mathbf{b}}}$ . The goal of the integer ambiguity estimation is thus to improve the precision of the baseline estimates. However, when the ambiguities are fixed to incorrect values, the fixed baseline solution may be wrong and it will be difficult to detect this error. For that reason it is important to have a-priori information on the probability of correct integer ambiguity estimation.

### 2.2.3. Success rate

When the ambiguities are fixed to incorrect values, the fixed baseline solution may be wrong and it will be difficult to detect the errors. So, it is important to estimate the integer ambiguities correctly. The ambiguity success rate is the probability that the integer ambiguities are

correctly estimated. Its lower bound is given as [13,15]:

$$P(\check{\mathbf{z}} = \mathbf{z}) \geq \prod_{i=1}^n \left[ 2\phi\left(\frac{1}{2\sigma_{z_i}}\right) - 1 \right] \quad (22)$$

Where  $n$  is the number of ambiguities and

$$\phi(x) = \int_{-\infty}^x \frac{1}{\sqrt{2\pi}} \exp\left\{-\frac{1}{2}z^2\right\} dz. \quad (23)$$

The standard deviation  $\sigma_{z_i}$  is the square root of the conditional variance of the  $i^{\text{th}}$  ambiguity (conditioned on the previous  $l = 1, \dots, i-1$  ambiguities). It can be obtained from the diagonal matrix  $\mathbf{D}$  after an  $\mathbf{LDL}^T$ -decomposition of the matrix  $\mathbf{Q}_{\check{\mathbf{z}}}$ . This matrix can be computed without the need of actual observations, so that also the success rate can be considered as a design parameter. It should be sufficiently high, i.e. very close to unity, in order to guarantee that the ambiguities will be fixed to their correct values. The ambiguity success rate can be obtained once the functional model, the stochastic model, and the integer ambiguity estimator are known. Although more appropriate geometry will result in a better rate of success in ambiguity resolution, but as mentioned before, unlike DOPs, this measure depends on other factors such as the precision of measurements and the adopted algorithm for ambiguity resolution. Therefore, the rate of success in ambiguity resolution is also used to evaluate the capability of carrier-phase-based positioning by the constellation proposed in this research. Further information about ambiguity success rate can be found in Refs. [15,16,20].

### 2.3. Constellation value

The positioning performance of a constellation can be measured in terms of positioning accuracy such as the PDOP for a user on the ground at a specific time located in a single point. In this study the constellation value (CV) is applied to measure the positioning performance for the proposed constellations as well. In fact, The CV can reflect the characteristic of satellite-user geometry and continuous availability. The CV is defined as the fraction of the Earth's surface, averaged over time, where a characteristic of the constellation does not exceed a certain number [21]:

$$CV = \frac{\sum_{t=t_0}^{t_0+\Delta T} \sum_{i=1}^L \text{bool}(C_{t,i} \leq C_{\max}) \times \text{area}_i}{\Delta T \times \text{Area}} \quad (24)$$

where  $\Delta T$  is the simulation time,  $L$  is the number of areas,  $\text{bool}(X)$  is the Boolean Function,  $\text{Area} = \sum_{i=1}^L \text{area}_i$  is the total simulation area,  $\text{area}_i$  is the area of  $i^{\text{th}}$  grid and  $C$  can be any performance measure for positioning such as PDOP or the number of epochs required to reach 99% ambiguity success rate that are performed further.

### 3. Constellation optimization

In this research, GA is applied to obtain the constellation parameters. GA is an optimization technique which is based on searching in the solution space in order to find an optimal solution or the one which possesses the desired qualifications. GA imitates natural biological evolution based on 'survival of the best' rule. In this technique, each solution in the search space is represented by a chromosome which is

typically a binary encoded string. A set of chromosomes makes up a population and the first population is generally generated randomly. The evolutionary process uses successive iterations of selection, crossover and mutation. By the act of these genetic operators a new population with the same number of chromosomes is reproduced to improve the quality of the candidate solutions represented as the population. So, a fitness function must be devised helping the selection from the current population based on fitness modified through crossover and mutation operations to form a new population [5]. The new population is used as next generation and this trend will continue until the stop condition is established. The stop condition can be a maximum number of generations reach, a satisfactory fitness level achievement for the population or reach a certain threshold number for iterations without any improvement in the fitness value. In this research, initial orbital parameters including the right ascension of ascending node, the orbital inclination, the eccentricity and the mean anomaly are represented by 8 bit. Since constellations are based on geosynchronous satellites, the semi major axis is equal to  $a = 42164.17$  Km and the argument of perigee is assumed equal to 270-deg. Therefore, the number of unknown parameters reduces from 6 to 4 per satellite.

Due to the large number of variables involved in the problem, in the absence of suitable constraints, solving the problem would be either a time consuming process or impossible by GA. For simplicity, a constellation is typically made up satellites which possess similar orbital parameters such as altitude, inclination, eccentricity and phasing. To this end, usually in the optimization problem of constellation design for Medium Earth Orbiting (MEO) and Low Earth Orbiting (LEO) satellites, prominent patterns such as Walker Patterns, are regarded as the baseline [22]. This will help to reduce number of parameters.

Geosynchronous satellites revolve around the Earth with a period of one sidereal day. Seen from a fixed point on the Earth, their trace paths in the sky repeat every day forming simple and meaningful analemmas. They are generally roughly elliptical, teardrop shaped, or figure-8 in shape. Their shapes and dimensions depend on the orbital parameters. Instead of using constellation patterns, each satellite is placed in an orbit so as to pass over the same ground track at a constant interval in a group with other satellites. Such constellations have been seen before, in QZSS using three satellites, each 120-deg apart, in highly-inclined orbits. This constellation is shown in Fig. 1. Also, three of the seven satellites in the IRNSS will be placed in GEO and four in IGSO. The IGSO satellites shall orbit the Earth with identical ground traces 180-deg apart.

This constraint helps reach better solutions leading to constellations uniformly distributed across the region of interest and makes the GA more practical. This is satisfied if the following relations are valid for the orbital parameters of the satellites with the same ground track:

$$\varphi = 360^\circ / N \tag{25}$$

$$\omega_1 = \omega_2 = \dots = \omega_N \tag{26}$$

$$i_1 = i_2 = \dots = i_N \tag{27}$$

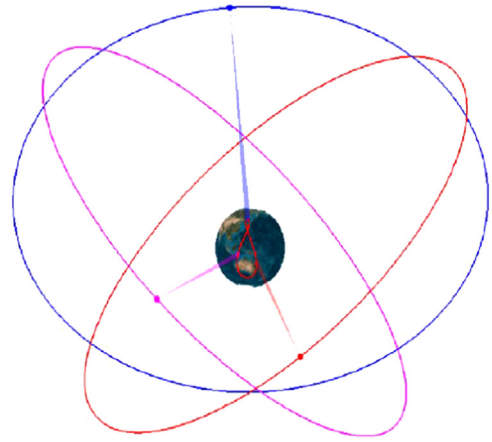


Fig. 1. QZSS satellites constellation passing over the same ground track at a constant interval [23].

$$e_1 = e_2 = \dots = e_N \tag{28}$$

$$\Omega_i = \Omega_j \pm k \varphi \quad i, j = 1, 2, \dots, N \quad k_z \neq 0 \quad i \neq j \tag{29}$$

$$M_i = M_j \pm k \varphi \quad i, j = 1, 2, \dots, N \quad k_z \neq 0 \quad i \neq j \tag{30}$$

$$\Omega_i + M_i = \Omega_j + M_j \quad i, j = 1, 2, \dots, N \tag{31}$$

where N is number of satellites with an identical ground track,  $\varphi$  is the constant interval of satellites,  $\Omega$  is the right ascension of ascending node,  $i$  is the orbital inclination,  $e$  is the eccentricity,  $\omega$  is argument of perigee and M is mean anomaly.

The area is divided into square cells, each encompassing 5-deg in latitude and 5-deg in longitude and the fitness function is defined as follows:

$$Fitness\ Function = \sum_{t=1}^T \sum_{i=1}^I PDOP_{i,t} / (T \times I) \tag{32}$$

Where  $i$  and  $t$  are the cell and time index and  $T$  and  $I$  are the total number of epochs and cells respectively. Since the optimization is based on minimum of navigation error for the period, satellite systems are simulated for 24 hours (i.e. a full period of satellites). PDOPs are computed in each cell by a time interval of 60 min.

6 and 7 satellites are chosen as the initial number of utilized satellites in the system. Since placing all satellites of the constellation in a group to pass over the same ground track at a constant interval, may not lead to the best solution of the problem, satellites are divided into groups so that each satellite has the same ground track just with other members of the group and orbits at a constant interval relative to other satellites of the group by applying Eqs. (25–31). This constraint reduces number of parameters under optimization from 4 per satellite to 4 per group (i.e. per distinct ground track). Whereas number of groups and also number of satellites of each group are questions of this research, all possible arrangements are optimized and compared. Table 1 and Table 2 report on the arrangements made and the obtained optimum fitness value of each arrangement, for 6 and 7 satellites respectively. To show

the arrangements, each number indicates the number of satellites in the group as they are separated by dash lines.

**Table 1**

The arrangements made and the best obtained fitness values for 6 satellites.

arrangement	4-fold minimum visibility anytime and anywhere in the region	Optimum fitness value
6	Not achieved	–
5-1	Achieved	1.97
4-2	Achieved	1.93
3-3	Not achieved	–
4-1-1	Achieved	1.90
3-2-1	Achieved	1.77
2-2-2	Not achieved	–
3-1-1-1	Achieved	1.76
2-2-1-1	Achieved	1.84
2-1-1-1-1	Achieved	1.91

**Table 2**

The arrangements made and the best obtained fitness values for 7 satellites.

arrangement	4-fold minimum visibility anytime and anywhere in the region	Optimum fitness value
7	Achieved	2.21
6-1	Achieved	1.68
5-2	Achieved	1.47
4-3	Achieved	1.45
5-1-1	Achieved	1.41
4-2-1	Achieved	1.43
3-3-1	Achieved	1.50
3-2-2	Achieved	1.42
3-2-1-1	Achieved	1.40
4-1-1-1	Achieved	1.44
2-2-2-1	Achieved	1.43
3-1-1-1-1	Achieved	1.48
2-2-1-1-1	Achieved	1.55
2-1-1-1-1-1	Achieved	1.54

**Table 3**

The optimum constellation parameters with 6 satellites.

Satellite Number	$a$ (m)	$i$ (degree)	$e$	$\Omega$ (degree)	$\omega$ (degree)	$M$ (degree)
1	42,164,170	57.863	0.400	196.235	270.000	290.921
2	42,164,170	57.863	0.400	316.235	270.000	170.921
3	42,164,170	57.863	0.400	76.235	270.000	50.921
4	42,164,170	2.549	0.009	81.882	270.000	23.706
5	42,164,170	0.510	0.008	264.000	270.000	250.804
6	42,164,170	3.823	0.080	251.294	270.000	236.255

**Table 4**

The optimum constellation parameters with 7 satellites.

Satellite Number	$a$ (m)	$i$ (degree)	$e$	$\Omega$ (degree)	$\omega$ (degree)	$M$ (degree)
1	42,164,170	69.333	0.737	336.000	270.000	161.745
2	42,164,170	69.333	0.737	96.000	270.000	41.745
3	42,164,170	69.333	0.737	216.000	270.000	281.745
4	42,164,170	5.647	0.047	127.059	270.000	339.902
5	42,164,170	5.647	0.047	307.059	270.000	159.902
6	42,164,170	5.961	0.043	83.294	270.000	71.118
7	42,164,170	7.843	0.043	237.176	270.000	275.274

As the results report, two constellations propose the best results in terms of the fitness value among the others. These constellations are chosen as the best solutions, 3-1-1-1 for 6 satellites and 3-2-1-1 for 7 satellites. The resulting orbital parameters of these constellations are listed in Tables 3 and 4 for 6 and 7 satellites at 14:50 UTC, respectively.

The constellations' ground tracks composing of 6 and 7 satellites are shown in Fig. 2 and Fig. 3 respectively. The results demonstrate a tendency to use a combination of near GEO and IGSO satellites. The first constellation uses 3 orbits with low eccentricity which distributes the 3 satellite across the region longitude near the Equator while in the second constellation 4 satellites are placed in either side of this region, two by two. The other difference is the eccentricities obtained for IGSO satellites. As seen, the second constellation uses a highly eccentric orbit that spends majority of its time in the neighborhood of apogee. For this orbit, the satellite is over the northern hemisphere. As the altitude of apogee is high, it will therefore, for a considerable period around the apogee, have an excellent visibility from the northern hemisphere, from the region, from the northern Europe, Russia and China as well. The three IGSO satellites of first constellation are over the northern hemisphere almost 18 h of their daily orbital period while this value for the second constellation is 22 h.

#### 4. Performance evaluation

Because of the lack of regional satellite systems, GPS is the only prominent and popular tool for navigation and positioning purposes in the Middle East. Since we expect the system to operate independently, performance of the proposed constellation is compared with GPS in the study region. For this purpose, simulated data are produced. This includes simulating the satellites' motion and analyzing the performance of the system. The scheme applied to generate GPS satellite positions from Keplerian elements or YUMA almanacs is shown in Fig. 4.

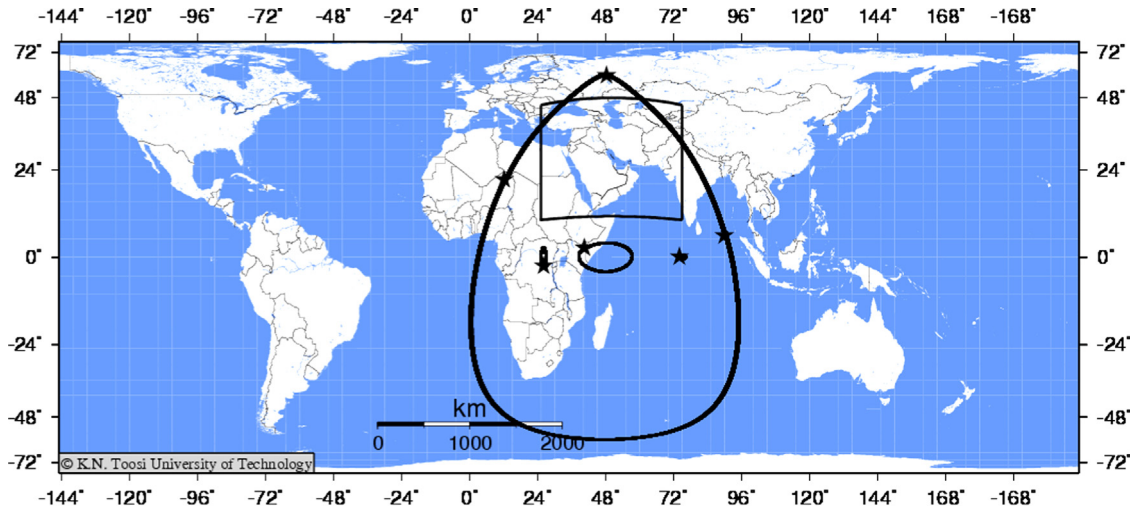


Fig. 2. Ground track of the constellation with 6 satellites (First constellation).

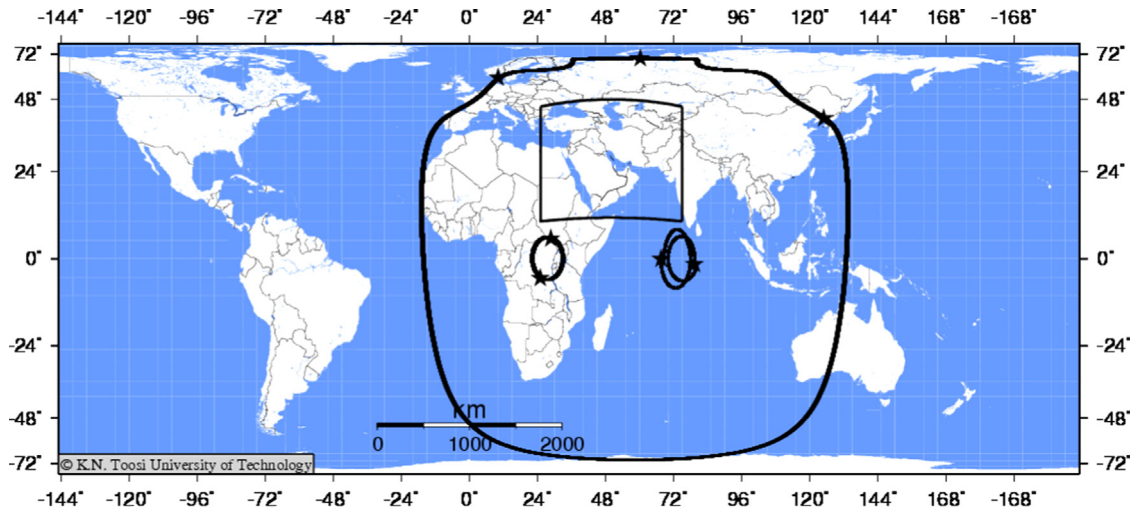


Fig. 3. Ground track of the constellation with 7 satellites (Second constellation). Distortions in the satellite ground tracks with larger eccentricities is due to the utilized map projection.

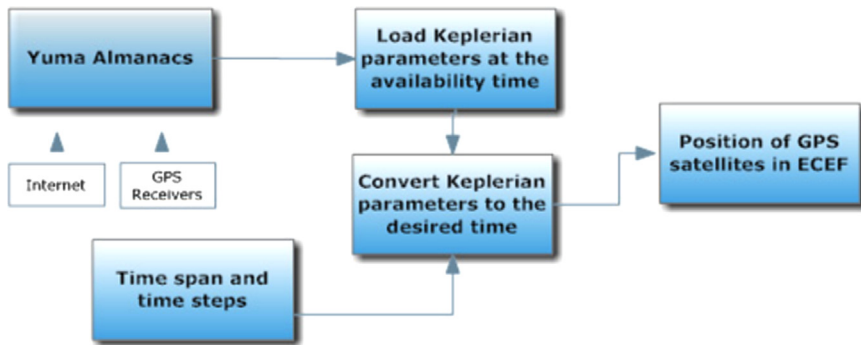


Fig. 4. Scheme to generate satellite positions from Keplerian elements.

Starting with Keplerian Orbital elements, the GPS and proposed constellation satellites' position are calculated in an Earth Centered Earth Fixed frame (ECEF), see [24] for further details. It should be noted that all simulation time spans start from 14:50 UTC in 27th of January 2014 for 24 h (i.e. a whole period time span).

The visibility of satellites as well as the code and phase observation based positioning performance has been taken into account. The study area is divided to small cells with a size of one degree per side. Visibility is then computed at the central point of the cells. Fig. 5 displays the simulation results for the average visibility of the satellites for the first, second and the GPS constellations,

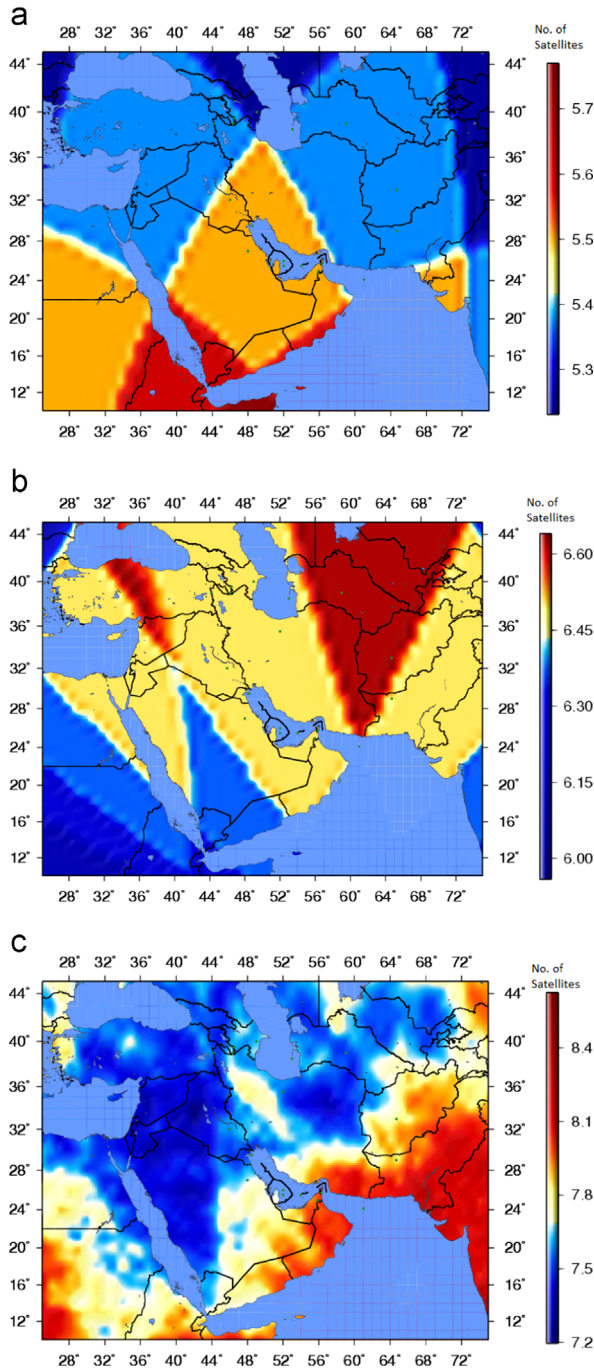


Fig. 5. Average visibility for the first (a) second (b) and GPS (c) constellations.

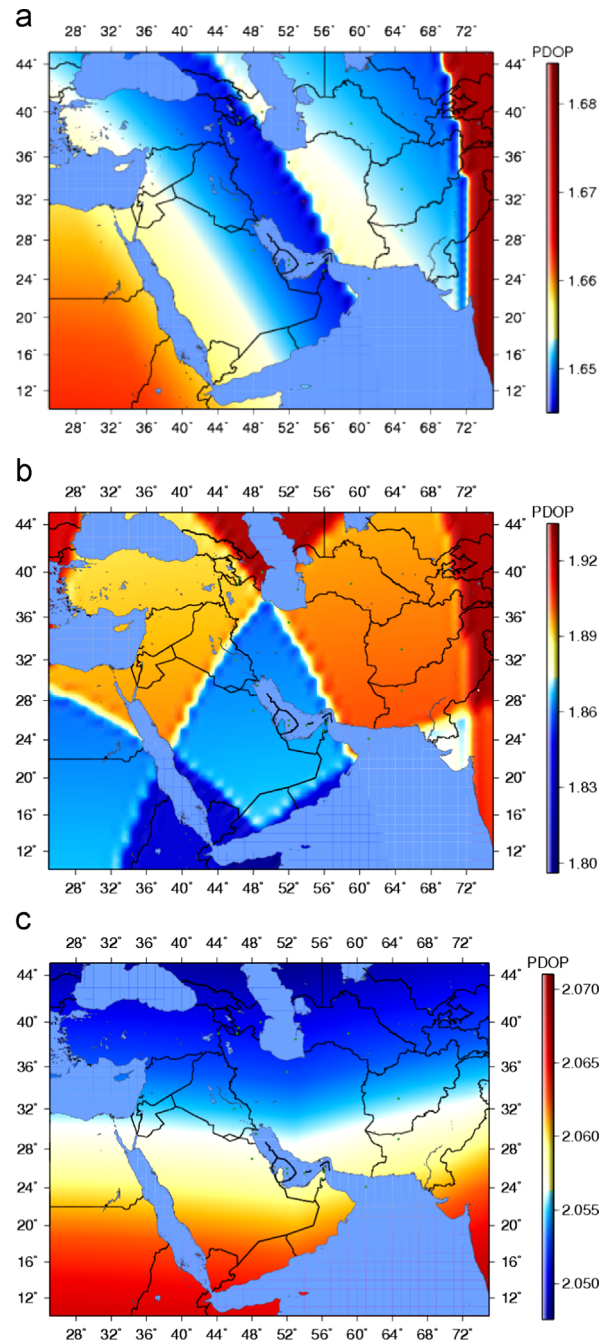


Fig. 6. Minimum (a), average (b) and maximum (c) of the PDOPs for the constellation with 6 satellites.



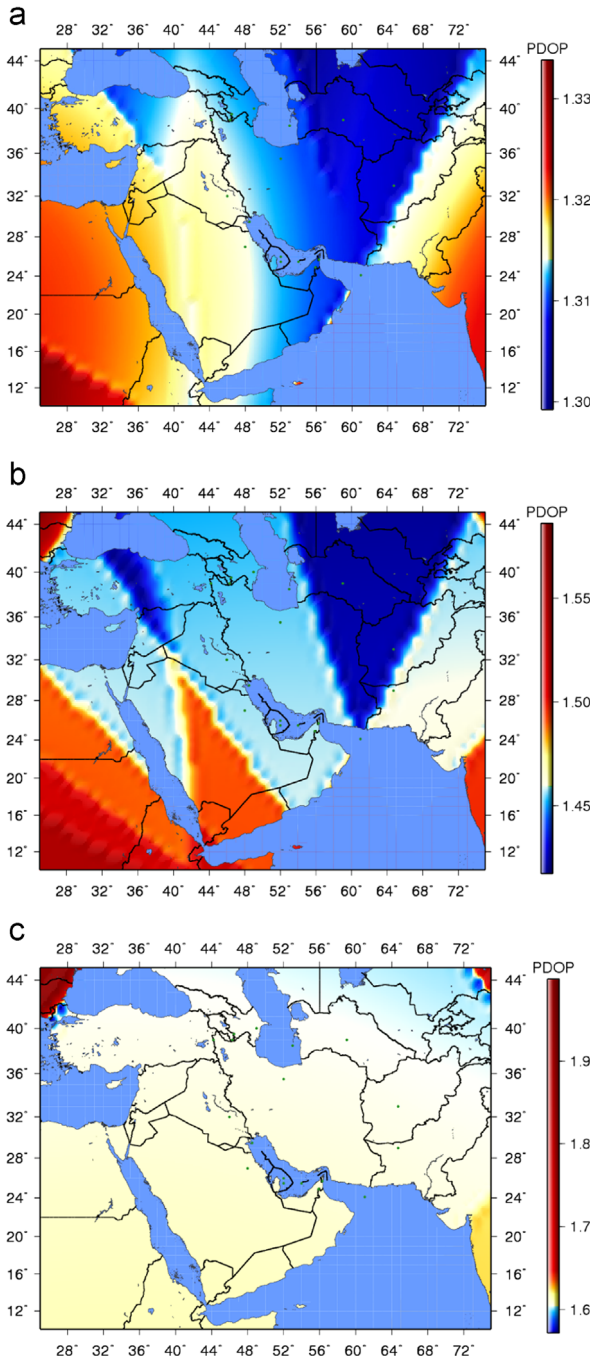


Fig. 7. Minimum (a), average (b) and maximum (c) of the PDOPs for the constellation with 7 satellites.

respectively. The masking angle is assumed to be equal to 15 degrees here.

According to the obtained results and similar to GPS, for both of the proposed constellations a minimum of 4 satellites is visible throughout the day, anywhere in the study area. Therefore, the application of the GA algorithm provides

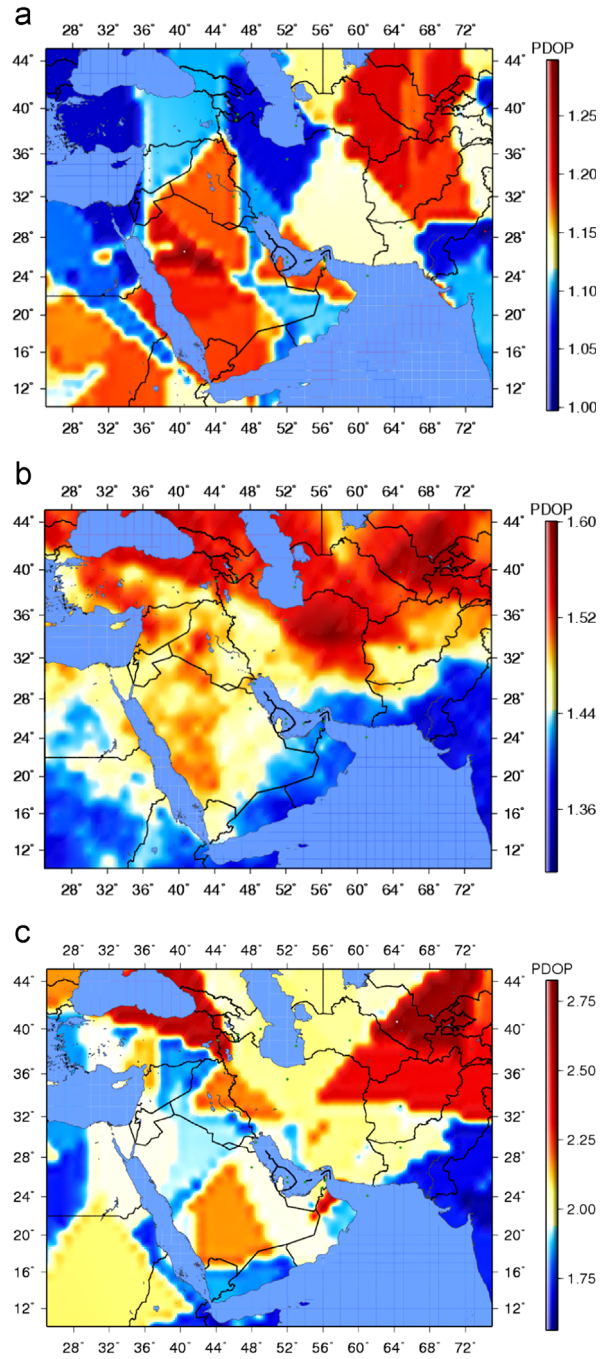


Fig. 8. Minimum (a), average (b) and maximum (c) of the PDOPs for GPS.

a uniform distribution of the satellites across the study region.

The accuracy of positioning is analyzed using minimum, average and maximum values of the PDOP parameter computed for every cell mentioned above. Estimated PDOPs are shown as a function of geographic location in Figs. 6, 7 and 8 for the first, second and the GPS constellations, respectively

**Table 5**  
PDOP based CVs for the constellations.

$PDOP_{max}$	First constellation	Second constellation	GPS
1.25	0.000	0.000	0.138
1.50	0.000	0.461	0.664
1.75	0.377	0.998	0.915
2.00	0.547	1.000	0.972
2.25	1.000	1.000	0.994

To report the obtained results, constellation value is computed using different thresholds of  $PDOP_{max}$ , see Table 5 for details. The adopted values for  $PDOP_{max}$  are based on the estimated maximal dilution of precision in each constellation above. For both of the proposed constellations, in navigation with a code similar to the GPS coarse acquisition code, it is not possible to achieve a positioning accuracy better than  $CPE = 3.75$  meters, where  $CPE$  is the Circular Positioning Error (CPE) equivalent to  $PDOP_{max} = 1.25$ . This is also valid for the first constellation when  $PDOP_{max} = 1.5$ . Nevertheless, the navigation error is almost equal to  $CPE = 4.5$  meters in 46% of the study area in 24 h a day for the second constellation of this research. For  $5.25 \leq CPE \leq 6.75$  ( $1.75 \leq PDOP \leq 2.25$ ), the performance of the second constellation is not only comparable but also slightly better than the GPS in the study area of this research. Following previous results, the performance of the first constellation is again obviously poorer as compared to the others. This is naturally due to the smaller number of satellites in this constellation.

The circular positioning error of 6.75 m is quite adequate for navigation purpose. Therefore, constellation one is not inferior to the other constellations when navigation is assumed to be the sole application in this research. Nevertheless, in precise positioning using carrier phase measurements, constellation two is obviously superior to the others. The CPE reduces to 3.5 mm in almost 100% of the study area during the day.

Next, the number of measurement epochs required to reach a fixed solution is analyzed. For this purpose, measurement epochs are sequentially incorporated in the estimation of the success rate parameter. The success rate of 99% is used to decide on the required number of measurement epochs. Through this process, the minimum length of measurements to be used in order to obtain a fixed solution is derived. Lower number of measurement epochs required to achieve a fixed solution is a measure for the comparison of the performance of the satellite systems in this research. To compute the rate of success in ambiguity resolution a signal structure similar to the GPS has been taken into account. Moreover, a stationary baseline model is used. The L5 observations were not considered in the simulation process. In addition, the accuracies of the code and phase measurements were taken as 0.300 and 0.003 m respectively [25]. The epoch rate is 30 s here. Using the weighted-model for the baselines of almost 15 km long, the rate of success in ambiguity resolution is computed in each cell during the day. Again, the minimum, average and maximum number of the required epochs is shown in Figs. 9–11 for constellations with 6 and 7 satellites and the GPS, respectively.

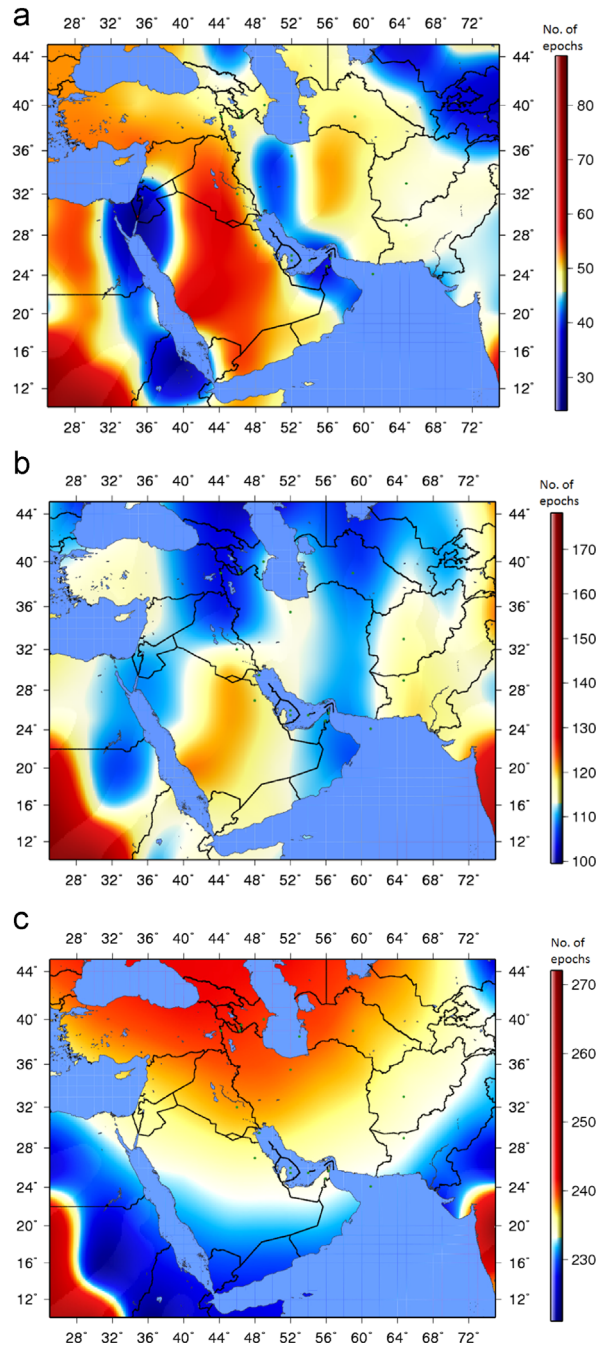


**Fig. 9.** Minimum (a), average (b) and maximum (c) number of required epochs to achieve the success rate of 99% by the constellation with 6 satellites.

Comparing Figs. 9 and 6, Figs. 10 and 7 as well as Figs. 11 and 8 it can be seen that decreasing PDOP decreases the required time for ambiguity resolution. This is a proof for the numerical computations of this research. Since the required number of measurement epochs for the successful resolution of the ambiguity parameters depends on the number of carrier phase measurements in each epoch, the adopted threshold value is met sooner for the GPS system as compared to the other constellations of this research. As a

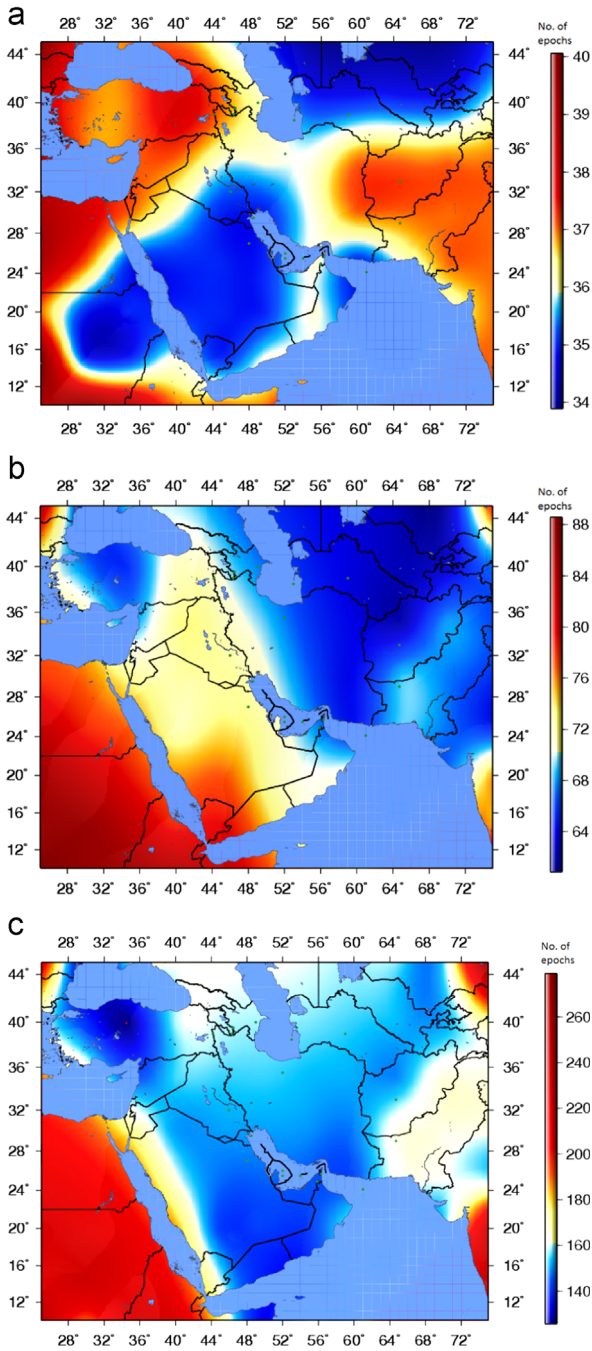


**Fig. 10.** Minimum (a), average (b) and maximum (c) number of required epochs to achieve the success rate of 99% by the constellation with 7 satellites.

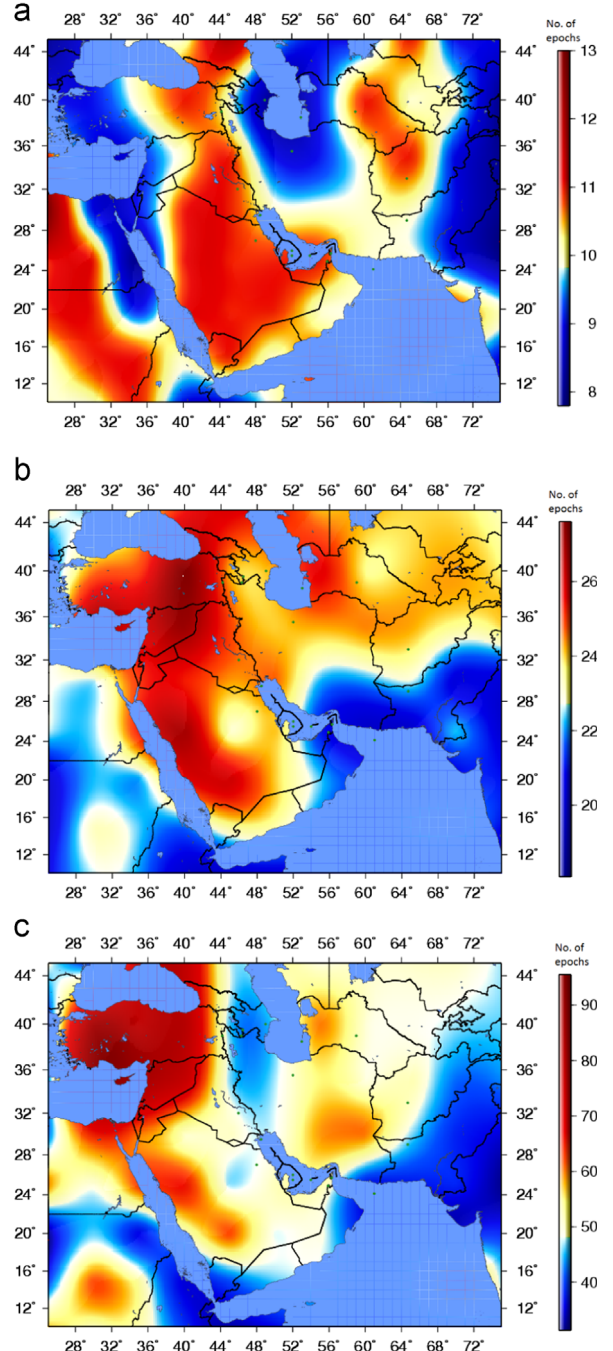


**Fig. 11.** Minimum (a), average (b) and maximum (c) number of required epochs to achieve the success rate of 99% by GPS.

result, the number of satellites plays an important role in the required time for ambiguity resolution.

To discuss on the obtained results in further detail, constellation values are computed using different values for the required time span in ambiguity resolution ( $epoch_{max}$ ). Table 6 provides the corresponding details. According to the obtained results, 30 min of measurements to the GPS satellites can guarantee the correct resolution of the initial phase

ambiguity parameters whereas, the corresponding probability is as much as 42% and 17% for the second and first constellations, respectively. The required time for a correct resolution of ambiguity parameters increases to 90 and 135 min for the second and first constellations of this research. This implies that due to utilization of smaller number of satellites in this research; the required measurement time for a fixed solution is 3 to 4.5 times worse than the GPS. Implementing

**Table 6**

CVs based on the required number epochs in an ambiguity fixed solution.

$epoch_{max}$	First constellation	Second constellation	GPS
30	0.002	0.000	0.779
60	0.174	0.426	0.991
90	0.356	0.761	1.000
120	0.544	0.907	1.000
150	0.745	0.961	1.000
180	0.860	0.987	1.000
210	0.925	0.991	1.000
240	0.982	0.999	1.000
270	1.000	1.000	1.000
300	1.000	1.000	1.000

geosynchronous satellites highly increases the system's cost. Therefore, the application of the second constellation is reasonable if precise positioning is considered as one of the main objectives in design and development of a satellite navigation mission.

## 5. Conclusions

This work uses genetic algorithm to propose a constellation design for a satellite navigation system in the Middle East region. Since the coverage as a criterion for constellation design is not sufficient enough to guarantee a good navigation service, positioning with pseudo-range and carrier phase has been discussed and the PDOP is collected as the optimization criterion. The preliminary results on the basis of PDOP, do illustrate that the performance of the constellation with 7 satellites is not far from GPS in the Middle East region. The existing similarity between the spatial distribution of the PDOP values for the constellations of 6 and 7 satellites is an indication for appropriateness of GA as an optimization tool of this work. The required number of measurement epochs for a successful resolution of the initial phase ambiguities when carrier phases are used is also analyzed. This is an important measure when precise positioning is taken as a main aim in the design and development of a navigation satellite system. Hence, the corresponding probability, which is also known as a success rate, has been assumed to be 0.99. It is shown that the number of utilized satellites plays an important role in the required time for ambiguity resolution. Although the proposed constellations do not perform as well as GPS, they can be considered as optimal constellations for an independent regional navigation satellite system. Regarding to the project budget, objectives and advantages of using more satellites, a decision can be made on the optimum design. However, if precise positioning is taken into account, the application of 7 satellites is inevitable. As a general conclusion, GA is capable for geosynchronous satellite constellation optimization for positioning purposes.

## Acknowledgements

Authors would like to express their very great appreciation to Hossein Etemadfar, Ph.D. student in Geodesy

Department of K.N. Toosi University of Technology, for sharing his valuable and constructive experiences.

## References

- [1] S. Clark, Japan to build fleet of navigation satellites, *Space Flight Now*, 2013.
- [2] A. Singh, S. Saraswati, India heads for a regional navigation satellite system, *Coordinates 2* (2006) 6–8.
- [3] CSNO, BeiDou Navigation Satellite System Signal in Space Interface Control Document (Test Version), China satellite navigation office December 2011, <<http://www.beidou.gov.cn/attach/2011/12/27/201112273f3be6124f7d4c7bac428a36cc1d1363.pdf>>.
- [4] L. Feng, W. Zhou, X. Wu, Realization of high-precision relative positioning using beidou regional navigation satellite system, in: J. Sun, W. Jiao, H. Wu, C. Shi (Eds.), *China Satellite Navigation Conference (CSNC) 2013 Proceedings*, Springer, Berlin Heidelberg, 2013, pp. 197–209.
- [5] D. Goldberg, J. Holland, Genetic algorithms and machine learning, *Mach. Learn.* 3 (1988) 95–99.
- [6] C.M. Fonseca, P.J. Fleming, *Genetic Algorithms for Multiobjective Optimization: Formulation Discussion and Generalization*, ICGA, 1993, 416–423.
- [7] W.A. Crossley, E.A. Williams, Simulated annealing and genetic algorithm approaches for discontinuous coverage satellite constellation design 32 (2000) 353–371 *Eng. Optim.* 32 (2000) 353–371.
- [8] T. Ely, W. Crossley, E. Williams, Satellite constellation design for zonal coverage using genetic algorithms, *J. Astronaut. Sci.* 47 (1999) 207–228.
- [9] M. Asvial, R. Tafazolli, B.G. Evans, Satellite constellation design and radio resource management using genetic algorithm, *Communications, IEE Proceedings* 151 (2004) 204–209.
- [10] O. Abdelkhalik, A. Gad, Optimization of space orbits design for Earth orbiting missions, *Acta Astronaut.* 68 (2011) 1307–1317.
- [11] K. Yan, F. Yang, C. Pan, J. Song, F. Ren, J. Li, Genetic algorithm aided gray-APSK constellation optimization, in: *Wireless Communications and Mobile Computing Conference (IWCMC)*, 2013 9th International, IEEE, 2013, pp. 1705–1709.
- [12] P. Misra, P. Enge, *Global Positioning System: Signals, Measurements and Performance*, Second Edition, Ganga-Jamuna Press, Lincoln, MA, 2006.
- [13] P. Teunissen, P. Joosten, C. Tiberius, A comparison of TCAR, CIR and LAMBDA GNSS ambiguity resolution, in: *Proceedings of the 15th International Technical Meeting of the Satellite Division of the Institute of Navigation (ION GPS-2002)*, 2002, pp. 2799–2808.
- [14] P. De Jonge, C. Tiberius, The LAMBDA method for integer ambiguity estimation: implementation aspects, *Publications of the Delft Computing Centre, LGR-Series*, Delft, Netherlands, 1996.
- [15] P.J. Teunissen, Success probability of integer GPS ambiguity rounding and bootstrapping, *J. Geod.* 72 (1998) 606–612.
- [16] S. Verhagen, Performance analysis of GPS, Galileo and integrated GPS-Galileo, in: *Proceedings of the 15th International Technical Meeting of the Satellite Division of the Institute of Navigation (ION GPS-2002)*, 2002, pp. 2208–2215.
- [17] P.J. Teunissen, A. Kleusberg, P. Teunissen, *GPS for Geodesy*, Springer, Berlin, 1998.
- [18] P. Teunissen, Least-squares estimation of the integer GPS ambiguities, in: *Invited lecture, section IV theory and methodology*, IAG General Meeting, Beijing, China, 1993.
- [19] D. Odijk, Fast precise GPS positioning in the presence of ionospheric delays, *Delft University of Technology, Department of Mathematical Geodesy and Positioning*, Delft, Netherlands, 2002.
- [20] P. Joosten, C. Tiberius, Fixing the ambiguities: are you sure they're right? *GPS World* 11 (2000).
- [21] G. Perrotta, S.D. Girolamo, New Navigation Satellite System Based on Intermediate Circular Orbits, *J. spacecr. Rockets* 35 (1998) 792–796.
- [22] J. Walker, Satellite constellations, *J. Br. Interplanet. Soc.* 37 (1984) 559–572.
- [23] N. Inaba, A. Matsumoto, H. Hase, S. Kogure, M. Sawabe, K. Terada, Design concept of Quasi Zenith Satellite System, *Acta Astronaut.* 65 (2009) 1068–1075.
- [24] G. Xu, *GPS: theory, algorithms, and applications*, Springer-Verlag, Berlin Heidelberg, 2007.
- [25] S. Verhagen, A New Software Tool-Studying the Performance of Global Navigation Satellite Systems, *GPS World*, 13, 2002, 60–65.